Scaling of Anisotropy in Hydromagnetic Turbulence

W. H. Matthaeus,[1] Sean Oughton,[2] Sanjoy Ghosh,[3] and Murshed Hossain[1]

[1]*Bartol Research Institute, University of Delaware, Newark, Delaware 19716-4793*
[2]*Department of Mathematics, University College London, London WC1E 6BT, United Kingdom*
[3]*Space Applications Corp., Vienna, Virginia 22180*

We present evidence that anisotropy of low frequency plasma turbulence scales linearly with the ratio of fluctuating to total magnetic field strength for a useful range of parameters, for incompressible, weakly compressible, and driven magnetohydrodynamic turbulence.   [S0031-9007(98)07008-2]

PACS numbers: 52.30.−q, 47.65.+a, 52.35.Ra, 95.30.Qd

Evidence accumulated over the past several decades indicates that a large-scale applied (dc) magnetic field imposes a preferred direction on turbulence, and thus plays an important role in plasma diffusion [1], energetic particle scattering [2], and plasma heating [3–5]. Each of these in turn may significantly influence large-scale flows and structure [6–8]. The interplay between turbulence and large-scale magnetic field suggests a crucial role of rotational symmetry or "geometry" of the fluctuations in many astrophysical plasma settings. There has been considerable recent interest in detection and understanding of anisotropy of fluctuations in solar, interplanetary, and galactic plasmas, and thus it would appear to be of importance to understand mechanisms that can produce and regulate anisotropy in fluid-scale plasma turbulence. In this Letter we show, using numerical solutions of magnetohydrodynamics (MHD), that anisotropy produced by spectral transfer scales in a systematic way with applied field strength. In particular, an angular measure of the anisotropy of the spectrum varies *linearly* with field strength over a useful range of applied field magnitudes. A simple argument, based upon the physics of reduced MHD [9–11], explains this scaling property as well as its saturation.

Within the MHD framework, anisotropy associated with a (uniform) dc magnetic field (B_0) may take a number of forms [12–14]. Here we are concerned specifically with dynamical development of spectral anisotropy due to asymmetry of nonlinear spectral transfer relative to the mean field direction [14,15]. This anisotropy is characterized by gradients across the mean magnetic field that are relatively larger than gradients along the field. Such features can be readily observed in fluctuations of plasma fluid velocity, magnetic field, and density, and have been observed in the solar wind [16–18], the solar corona [19], the interstellar medium [20,21], and in various laboratory plasma devices [22,23]. The limiting case, when all variations are perpendicular to the mean field, and the parallel coordinate is ignorable, is known as two-dimensional (2D) turbulence. The opposite limit, with perpendicular coordinates ignorable, often called "slab" symmetry, is traditionally employed in linear wave theory [2,16]. Turbulence that is "quasi-2D" is described by "reduced" MHD equations that emerge naturally in the theory of nearly incompressible MHD [24] for low plasma β.

It is well known that anisotropy can be generated robustly through rapid turbulent wave-vector–space spectral transfer in the directions transverse to the mean field [14]. Parallel spectral transfer is relatively suppressed, so the spectrum, especially at smaller scales, becomes progressively dominated by fluctuations with quasi-2D characteristics. This argument, which can be made explicit in terms of resonant triad couplings [14], supports the perspective adopted in derivations of the reduced MHD equations [9,10]. Development of anisotropic spectra through enhanced perpendicular spectral transfer has been observed in two- and three-dimensional simulations [25], and in both incompressible and compressible MHD simulations [26].

Here we employ numerical experiments with varying applied magnetic field strength to examine the scaling of MHD spectral anisotropy. MHD equations are solved in a periodic cube using Fourier spectral methods that have proved reliable in studies of hydrodynamic turbulence. For incompressible modeling, we solve the constant density incompressible MHD equations [25] in terms of the solenoidal fluid velocity **v** and fluctuating magnetic field **b**, with constant resistivity and viscosity coefficients, employing a Fourier-Galerkin method and the Orszag-Patterson transform method. For compressible numerical (pseudospectral) modeling [26], we solve the MHD Navier-Stokes equation for **v**, and vector potential equation for **a** (with $\mathbf{b} = \nabla \times \mathbf{a}$), with scalar dissipation coefficients. We adopt a polytropic equation of state and solve the corresponding continuity equation for mass density ρ. The polytropic model, frequently used in solar and heliospheric studies, is a computational convenience here, and is not expected to significantly impact our low Mach number compressible simulations. Initial (or steady) large-scale kinetic and magnetic Reynolds numbers are $R \sim 200$. Magnetic fields are in Alfvén speed units.

Standard numerical experiments examined here are the dissipative initial value problem (decay case) and the dissipative randomly driven problem that has attained a statistically steady state. Initial data and driving are band limited

and isotropic. In each case the (initial or steady) fluctuation energy per unit mass is approximately unity in the familiar dimensionless units, and the mean magnetic field $\mathbf{B}_0$—a uniform constant—is varied to examine its effects on spectral transfer and the development of anisotropy.

The degree of anisotropy is conveniently quantified [14,25,26] by the mean perpendicular wave number $\overline{k}_\perp = \sqrt{\langle k_\perp^2 \rangle}$ and mean parallel wave number $\overline{k}_\parallel = \sqrt{\langle k_\parallel^2 \rangle}$ where the Fourier wave vector $\mathbf{k}$ has components $k_\parallel$ and $\mathbf{k}_\perp$ parallel and perpendicular to $\mathbf{B}_0$, respectively. The mean value is taken with respect to a positive definite spectral density. For isotropy, $\overline{k}_\perp^2 = 2\overline{k}_\parallel^2$. Focusing on the vorticity, we have

$$\overline{k}_\perp = \sqrt{\frac{\Sigma k_\perp^2 |\boldsymbol{\omega}(\mathbf{k})|^2}{\Omega}}, \qquad (1)$$

where the vorticity $\boldsymbol{\omega} = \nabla \times \mathbf{v}$, $\Omega = \Sigma |\boldsymbol{\omega}(\mathbf{k})|^2$ is the enstrophy (mean square vorticity), and the sum is over all $\mathbf{k}$'s in the vorticity spectrum. It is also convenient to define an angular measure (or, *anisotropy angle*) θ_ω such that $\tan \theta_\omega = \overline{k}_\perp / \overline{k}_\parallel$. Anisotropy is indicated by systematic departures from the isotropic value $\theta_\omega = 54.7°$, or $\cos \theta_\omega = 0.577$. Dynamical development of quasi-2D anisotropy is indicated by growing θ_ω, and in general stronger anisotropy is seen for larger Reynolds numbers, stronger B_0, and at later times [14,25,26].

We now use simulation data to quantify variation of anisotropy with increasing field strength. For decaying turbulence, the anisotropy angle θ_ω is computed at a fixed turbulence "age"—at a time t_{60} at which the total incompressible MHD energy has decreased to 60% of its initial value. This ensures that different simulations are compared after passage of the same number of characteristic eddy turnover times [27]. Comparing runs at differing dc field strength but otherwise identical initial conditions shows that the computed $\cos \theta_\omega(t_{60}) \sim b/B$, the ratio of the field variance to the rms total magnetic field. This is illustrated in Fig. 1, for a series of runs with initial Reynolds number of 200, band limited initial data between dimensionless wave numbers k of $1 \leq k \leq 8$ and a resolution of 64^3 Fourier modes. The four incompressible runs at varying B_0 are fitted with a straight line, indicating an excellent fit to $\cos \theta_\omega \sim b/B$. Four additional points are shown in Fig. 1, obtained using a compressible MHD code but initial data that are identical (including uniform mass density) to the incompressible simulations shown in the same figure. In the compressible runs, the initial turbulent Mach number is 0.15. The close proximity of the compressible solutions to the incompressible ones is consistent with an interpretation that these solutions lie in the nearly incompressible regime [24]. The linear scaling of $\cos \theta_\omega$ illustrated in Fig. 1 is typical, and has been seen in a variety of other simulations that we have recently analyzed. Evidently, $\cos \theta_\omega \sim b/B$ is a fairly robust feature of decaying MHD turbulence.

To understand the physical basis for the observed scaling, we must first identify the types of nonlinear spectral
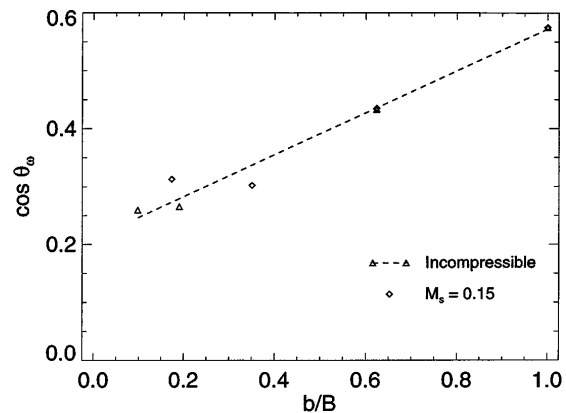

FIG. 1. Cosine of the anisotropy angle ($\cos \theta_\omega = \overline{k}_\parallel / \overline{k}$) for simulations with initial Reynolds number $R = 250$ and identical initial conditions with excitations confined to $k < 8$. Incompressible run data (triangles) are fitted with a straight line. Corresponding compressible run data are for initial turbulent Mach number $M_s = 0.15$.

transfer that remain strong in the presence of an applied magnetic field $\mathbf{B}_0$. Heuristically, the principal effect of strong $\mathbf{B}_0$ is to cause interference between the two Elsässer fields $\mathbf{z}^\pm = \mathbf{v} \pm \mathbf{b}$, which in the wave picture tend to propagate in opposing directions in the sense of Alfvén waves (in the incompressible limit). As noted by Kraichnan [3], this causes more rapid decay of triple correlations, thus suppressing spectral transfer. However, the magnitude of this effect varies considerably in accordance with the direction of the wave vectors involved, giving rise to anisotropy. We would expect that spectral transfer to higher $k_\parallel$ should be suppressed relative to transfer to higher $\mathbf{k}_\perp$, simply because higher $k_\parallel$ is associated with more rapid Alfvénic decorrelation, whereas transfer to higher $k_\perp$ is not. This is borne out in the simulation data as is illustrated in Fig. 2 where the behavior of mean $k_\parallel$ is contrasted with that of $k_\perp$ for simulations with $\mathbf{B}_0 = 0$ and 4. For the zero mean field case the transfer is consistent with isotropy. However, for $\mathbf{B}_0 = 4$ parallel transfer is essentially frozen out, suggesting that small-scale structures are mainly of a quasi-2D type and the cascade and dissipation processes are highly anisotropic [10,14].

Upon closer consideration we can see that there are two classes of interactions that are partially or fully exempt from the Alfvén wave decorrelation effect. The first class is typified by strictly 2D incompressible turbulence [28] in which all excitations have $k_\parallel = 0$ and the dc magnetic field becomes dynamically invisible. This class is appropriately broadened to include interacting triads of Fourier modes with $k_\parallel \neq 0$, but small enough that the corresponding Alfvén wave period is of order or longer than the typical nonlinear time. The latter class of quasi-2D turbulence is described by reduced MHD equations which have been derived by Montgomery under the equivalent assumption that the wave time scale remain order one as the dc field strength becomes large [10,15]. The second class of incompressible interactions that are
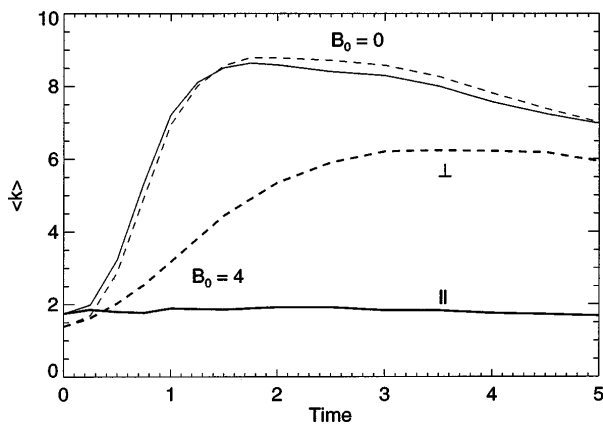
FIG. 2. Mean parallel components of wave vector parallel ($\parallel$) and perpendicular ($\perp$) to the dc magnetic field $\mathbf{B}_0$ for two of the incompressible runs shown in Fig. 1, labeled by their value of dc field strength B_0. The effect of B_0 is to suppress parallel transfer and initially slow perpendicular transfer.

insensitive to propagation effects are the resonant triads described by Shebalin *et al.* [14] in which at least one wave vector is associated with a zero frequency mode (or equivalently for the purposes of the present argument, a nearly zero frequency mode, i.e., a quasi-2D mode).

For both classes of interaction—2D and resonant—spectral transfer is in the direction towards higher $k_\perp$, not higher $k_\parallel$, and either class can explain the freeze-out of parallel transfer seen in Fig. 2. Interaction strengths are independent of B_0 for resonant couplings, and interacting triads of wave vectors are not restricted by the value of B_0 beyond the requirement that frequency and wave number matching conditions are met [14]. Thus, resonant transfer will not easily explain the linear scaling of anisotropy angle that seems to be a robust feature in simulation data for moderate values of $\delta B/B$.

The alternative scenario, that the observed scaling of anisotropy is associated with quasi-2D transfer, seems to readily provide an explanation. Adopting a (spectrally) local transfer hypothesis and assuming that nonresonant (or, zero-mode) transfer dominates over resonant transfer, we can estimate the region of wave vector space in which spectral transfer will be most vigorous. This region is defined by the requirement that the local nonlinear time $\tau_{\rm NL}$ is comparable to or smaller than the characteristic wave period τ_A, and thus nonlinear couplings within this region are relatively unaffected by Alfvénic propagation. The region of interest is prescribed by

$$|\mathbf{k} \cdot \mathbf{B}_0| < \frac{1}{\tau_{NL}(\mathbf{k})}, \qquad (2)$$

The quantity $\tau_{\rm NL}(\mathbf{k})$ is a dimensional estimate of the local eddy-turnover time, which is difficult to estimate without knowledge of the spectrum itself. However, since we expect that the time scale associated with decorrelation of the small-scale eddies is smaller than the large-scale eddy-turnover time, a modified and somewhat weaker restriction

is prescribed by

$$\cos \theta < \frac{1}{k\lambda} \frac{\delta B}{B_0}, \qquad (3)$$

where θ is the angle between $\mathbf{k}$ and $\mathbf{B}_0$ and λ is an energy-containing length scale such that the large-scale eddy-turnover time is $\delta B/\lambda$. Since $k\lambda \gtrsim 1$ for the scales of interest, this inequality is only meaningful when $\delta B/B_0 < 1$. In this parameter range we can approximately replace the value of dc field with the total rms field strength B, a replacement motivated by the reasoning [29] that large scale fluctuations induce wavelike propagation effects on the small scale fluctuations.

In order to estimate the anisotropy angle $\cos \theta_\omega$ associated with the vorticity, we note that the enstrophy spectrum (at sufficiently high Reynolds numbers) will be dominated by contributions from the cone of $\mathbf{k}$ space described by Eq. (3). Therefore, estimates of both mean parallel and mean perpendicular wave numbers will be essentially determined by contributions from this region. Figure 2 suggests that the parallel distribution of vorticity is essentially unchanged by spectral transfer. Perpendicular spectral transfer of the quasi-2D type is independent of B_0, and therefore $\langle k_\perp^2 \rangle$ will be determined by other factors such as the Reynolds numbers (or, perpendicular dissipation scale). The mean parallel wave number, on the other hand, must scale as $\overline{k}_\parallel \sim \delta B/B$ in accordance with Eq. (3). Consequently, $\cos \theta_\omega \sim \delta B/B$ for the parameter regime of interest.

Until this point we have discussed only simulations of decaying, dissipative MHD turbulence. However, the above reasoning also applies to driven dissipative steady state turbulence, with minor modification. Recently we have been able to verify using simulations that very similar linear scaling of $\cos \theta_\omega$ vs $\delta B/B$ is obtained for MHD turbulence driven by large-scale random driving. Figure 3 illustrates this result using four simulation runs in which the values of $\cos \theta_\omega$ are computed after the driven turbulence attains an approximately steady state.

The simulations have shown that spectral anisotropy behaves in a predictable manner as the mean magnetic field strength is varied. Linear scaling of anisotropy angle was seen for decaying turbulence and driven turbulence, and in both incompressible and low Mach number compressible MHD. However, we also expect there are parameter regimes in which this simple linear scaling fails, in particular at either very high or very low values of mean field strength. There is, for example, a suggestion in the simulations (Figs. 1 and 3) that saturation of anisotropy occurs at low b/B, as one would expect (see discussion above) when resonant spectral transfer is dominant. As yet, computations have not fully explored the weak and strong B_0 limits, but a possible basis for understanding the transition between such regimes has been discussed recently [11]. For the parameters explored in the simulations here, however, it appears that the use of reduced MHD, an entirely "zero frequency" description, is justified. In contrast, weak turbulence perspectives of the type that ignore "zero
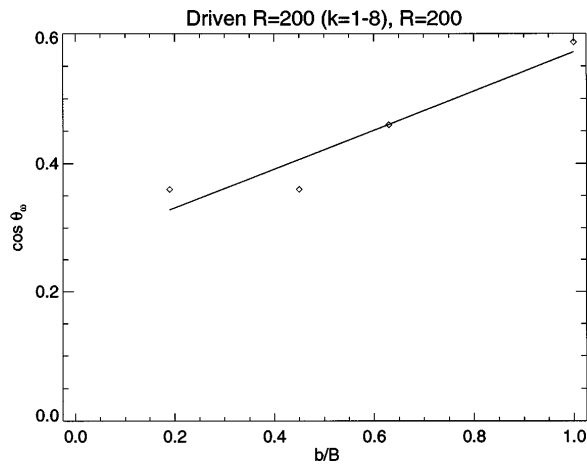
FIG. 3. Cosine of the anisotropy angle ($\cos\theta_\omega = \overline{k}_\parallel/\overline{k}$) for simulations with Reynolds number $R = 250$, randomly driven in the wave number band $k < 8$. Data (diamonds) are fitted with a straight line.

mode" effects [30,31] would seem inappropriate in the present case. In any case, quasi-2D excitations are essential also in the resonant transfer context [14,32,33]. One recent attempt to extend the weak turbulence approach to the strong regime [34] employed an assumption of "critical balance" that is essentially the limiting equality associated with Eq. (2). It is noteworthy that recognition of the importance of the near zero frequency dynamics, advanced originally in connection with the derivation of the reduced MHD equations [10], in the present context gives rise to a scaling that appears to be at odds with the conclusion of Goldreich and Sridhar [34] that $k_\parallel \sim k_\perp^{2/3}$.

We expect that anisotropy will also depend upon Reynolds numbers, bandwidths of initial data and/or forcing terms, and, possibly, anisotropic dissipation mechanisms [13]. In a subsequent publication we intend to explore some of these parameters, as well as the weak and strong B_0 limits.

Of the various applications discussed in the opening paragraph, perhaps the one that most clearly warrants a closing remark here is the issue of turbulent heating rates in MHD. Earlier numerical studies [5] noted MHD turbulence decay rates larger than the $\dot{E} \propto B_0^{-1}$ scaling associated with a naive extension of inertial range propagation effects [3] to the energy-containing range. It was proposed instead that $\dot{E} \propto (\delta B + B_0 \cos\theta_A)^{-1}$ might incorporate anisotropy effects through $\cos\theta_A$. Identifying $\cos\theta_A$ with the present $\cos\theta_\omega$ bolsters the expectation that MHD decay rates might frequently become independent of or weakly dependent upon B_0. This possibility, which may have important effects in a number of astrophysical settings, warrants further analysis.

[1] R. Balescu, H-D. Wang, and J. Misguich, Phys. Plasmas **1**, 3826 (1994).
[2] J. R. Jokipii, Rev. Geophys. Space Phys. **9**, 27 (1971).
[3] R. H. Kraichnan, Phys. Fluids **8**, 1385 (1965).
[4] H. K. Moffatt, J. Fluid Mech. (UK) **28**, 571 (1967).
[5] M. Hossain *et al.,* Phys. Fluids **7**, 2886 (1995).
[6] H. K. Moffatt, *Magnetic Field Generation in Electrically Conducting Fluids* (Cambridge University Press, New York, 1978).
[7] J. McKenzie, M. Banaszkiewicz, and W. I. Axford, Astron. Astrophys. **303**, L45 (1995).
[8] G. Zank, I. Cairns, and G. M. Webb, Adv. Space Res. (UK) **15**, 453 (1995).
[9] H. R. Strauss, Phys. Fluids **19**, 134 (1976).
[10] D. Montgomery, Phys. Scr. **T2/1**, 83 (1982).
[11] R. Kinney and J. C. McWilliams, J. Plasma Phys. **57**, 73 (1997); Phys. Rev. E **57**, 7111 (1998).
[12] E. N. Parker, *Spontaneous Current Sheets in Magnetic Fields* (Oxford Univ. Press, New York, 1994).
[13] D. C. Montgomery, J. Geophys. Res. **97**, 4309 (1992); S. Oughton, J. Plasma Phys. **56**, 641 (1996).
[14] J. V. Shebalin, W. H. Matthaeus, and D. Montgomery, J. Plasma Phys. **29**, 525 (1983).
[15] D. C. Montgomery and L. Turner, Phys. Fluids **24**, 825 (1981).
[16] J. W. Belcher and L. Davis, Jr., J. Geophys. Res. **76**, 3534 (1971).
[17] W. H. Matthaeus, J. W. Bieber, and G. P. Zank, Rev. Geophys. Supp. **33**, 609 (1995).
[18] J. Armstrong, W. Coles, M. Kojima, and B. Rickett, Astrophys. J. **358**, 685 (1990).
[19] R. R. Grall *et al.,* Nature (London) **379**, 429 (1996).
[20] J. Armstrong, J. Cordes, and B. Rickett, Nature (London) **291**, 561 (1981).
[21] K. Desai, C. Gwinn, and P. Diamond, Nature (London) **372**, 754 (1994).
[22] D. Robinson and M. Rusbridge, Phys. Fluids **14**, 2499 (1971).
[23] S. Zweben, C. Menyuk, and R. Taylor, Phys. Rev. Lett. **42**, 1270 (1979).
[24] G. P. Zank and W. H. Matthaeus, J. Geophys. Res. **97**, 17 189 (1992); Phys. Fluids A **5**, 257 (1993).
[25] S. Oughton, E. R. Priest, and W. H. Matthaeus, J. Fluid Mech. **280**, 95 (1994).
[26] W. H. Matthaeus, S. Ghosh, S. Oughton, and D. A. Roberts, J. Geophys. Res. **101**, 7619 (1996).
[27] W. H. Matthaeus, C. Smith, and S. Oughton, J. Geophys. Res. **103**, 6495 (1998).
[28] D. Fyfe and D. Montgomery, J. Plasma Phys. **16**, 181 (1976).
[29] A. Pouquet, U. Frisch, and J. Léorat, J. Fluid Mech. **77**, 321 (1976).
[30] S. Sridhar and P. Goldreich, Astrophys. J. **432**, 612 (1994).
[31] D. C. Montgomery and W. H. Matthaeus, Astrophys. J. **447**, 706 (1995).
[32] C. S. Ng and A. Bhattacharjee, Astrophys. J. **465**, 845 (1996).
[33] P. Goldreich and S. Sridhar, Astrophys. J. **485**, 680 (1997).
[34] P. Goldreich and S. Sridhar, Astrophys. J. **438**, 763 (1995).